DESIGN OF PUMP SHAFT TRAINS HAVING VARIABLE-SPEED ELECTRIC MOTORS

by

Arno Frei

Head, Mechanical Development Group

Sulzer Brothers Limited

Winterthur, Switzerland

Andrej Grgic

Supervisor, Department of Applied Mechanics for Rotating Electrical Machines

Brown Boveri & Company

Baden, Switzerland

Werner Heil

General Manager, Department AC and DC Machines for Industrial Application

Brown Boveri & Company

Baden, Switzerland

and

Armin Luzi

Research Engineer

Sulzer Brothers Limited

Winterthur, Switzerland

Arno Frei graduated in 1959 from St. Gall Technical College, Switzerland, with a degree in Mechanical Engineering. He joined Sulzer in 1966 and was first engaged in the design and development of primary recirculation pumps for nuclear power stations. After activities in the field of nuclear heat exchangers, he rejoined the pump division, where he has been Head of the Mechanical Development Group since 1978.

Andrej Grgic graduated in 1956 from the Technical Faculty of the University of Zagreb, Yugoslavia, with the Dipl.-Ing. degree in Mechanical Engineering, In 1960 he joined Brown Boveri & Company in Baden, Switzerland, as a Development Engineer. Since 1970 he has been supervisor of the Department of Applied Mechanics for Rotating Electrical Machines. He has published a number of papers in this subject area and is a member of various technical committees.

Werner Heil graduated in 1962 from Darmstadt Insitute of Technology, Federal Republic of Germany with the Dipl.-Ing. degree in Electrical Engineering (power & apparatus).

He joined Brown Boveri & Company in Baden, Switzerland, as a Design and Development Engineer in 1963. From 1970 to 1972, he taught design of electrical machines at the Brugg-Windisch Technical College, Switzerland. In 1972, he became Head of the Design Department DC and Special Machines and in 1978 he was appointed General Manager of the Deparment AC & DC Machines for Industrial Application.

Armin Luzi graduated in 1978 from Winterthur Technical College and in 1981 from the Federal Institute of Technology in Zürich, Switzerland, with a degree in Mechanical Engineering. Afterwards he joined the Laboratory for Vibrations and Acoustics at Sulzer, and has been employed as a Research Engineer since 1982. Mr. Luzi is engaged in experimental and theoretical research and development with many of Sulzer's products. He is working in the areas of rotordynamics and vibrations of pumps, weaving machines, turbocompressors and diesel engines.

ABSTRACT

With converter-fed variable-speed electric motors, pulsating torques inevitably occur in the air gap and can cause torsional oscillation in the whole shaft line. The origin and behavior of these torques and how to calculate them are described.

INTRODUCTION

During recent years, variable-speed electric motors have been increasingly used for drives in general, and in particular for pumps. This has been due to a combination of rising energy prices and the development of increasingly cost-effective electronic components.

These modern variable-speed drives offer the advantages of better process control and improved overall efficiency. As with all drive systems, they must be dynamically checked for torsional oscillation. In addition to the familiar processes of runup, short circuits and switching operations on the grid, etc., these drives are subject to pulsating torques caused by the static converter. The frequency of these pulsating torques is variable over a wide range, so that under certain conditions resonance operation at natural frequencies of the shaft line is practically unavoidable. Therefore, as reported herein, it has been attempted to explain the origin and behavior of these pulsating torques and how to calculate them.

SPEED CONTROL OF ELECTRIC MOTORS [1,2]

The essential elements of a variable-speed electric drive include a power supply network, a power pack with a control element, and an electric motor (Figure 1). Many different arrangements are possible (Table 1). The usual drive arrangement now consists of a static converter and a synchronous or asynchronous motor. The most usual combinations of converter and motor types for higher power rating (P > 1MW) are shown in Table 2 [3].

The speed of the synchronous motor is varied by controlling the stator frequency. The speed of an induction motor can be varied either through the stator frequency or the rotor frequency (only for wound rotors). The rotor-frequency control involves variation of the slip. The shaft speed is varied by phase-angle control or by means of a cascade circuit [4]. There are several types of stator-frequency control, depending on the supply arrangement (current, voltage) and type of commutation of the converter which feeds the motor (line-,load-, or self-commutated type). In all of the systems, the converter determines the frequency and voltage (or frequency and current) at the motor terminals.

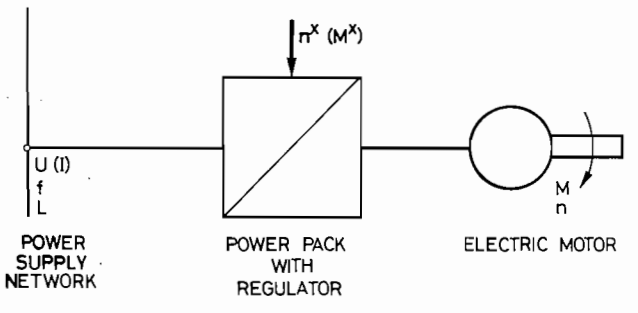

U:	Voltage	M:	Torque
I:	Current	n:	Speed (rpm)
f:	Frequency	n^X:	Setpoint for n
L:	Number of phases	M^X:	Setpoint for M

Figure 1. Basic Arrangement of a Drive Having Electrically Variable Speed.

Table 1. Examples of Design Solutions for Drives Having Electrically Variable Speed.

NETWORK VARIABLES	
– FREQUENCY:	50 Hz, 60 Hz, rarely direct-current (O Hz)
– VOLTAGE:	High voltage (U > 1 kV) Low voltage (U < 1 kV)
– NUMBER of CONDUCTORS:	Three-phase system, rarely two phases Single-phase system for traction applications
POSSIBLE POWER PACK ARRANGEMENTS	
– Adjustable transformer – Resistance cascade – Rotary converter – Static converter	
POSSIBLE ELECTRIC MOTORS	
– MOTOR WITH COMMUTATION:	Direct-current motor Three-phase commutator motor
– MOTOR WITHOUT COMMUTATION:	Synchronous motor Asynchronous motor – Slipring type – Squirrel-cage type

Table 2. Current Combinations of Converter and Motor Types for Variable-Speed Drives of over 1 MW.

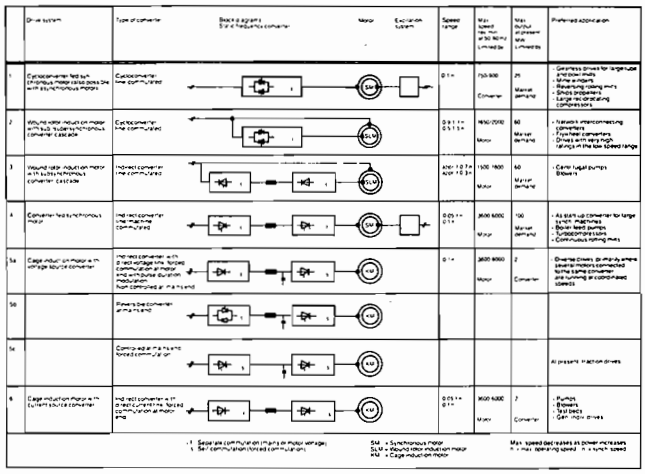

It is usually a converter-fed synchronous motor (Table 2, Case 4), which is used for boiler feed pump drives. This is because of the high power ratings and high speeds (n > 4000 cpm) required for this type of pump. For water supply systems, because of the commonly specified power ratings and speed range (n < 1800 cpm), subsynrhonous cascade converter systems are used (Table 2, Case 3). These selections are based on both technical and economic reasons [5, 6, 7, 8, 9, 10].

PULSATING TORQUES DURING NORMAL OPERATION

Static converters are controllable power supplies which have a discontinuous mode of operation. Depending on the type of converter, the complexity of the overall design, and the shaft speed, greatly differing periodic and transient distortions of the phase currents will occur. As a result, pulsating or surge torques

will occur in the air gap of the electric motor, and these can cause considerable torsional oscillations in the shaft line. In the air gap of three-phase motors, six-pulse converters will cause mainly pulsating torques at six times the stator feed frequency. In six-phase motors, the same power supply will cause pulsating torques at twelve times the feed frequency. The amplitudes of the latter torques will be only a fraction of those caused in three phase motors having six-pulse converters. In general, it can also be said that with *stator frequency control*, the frequency of the pulsating torques is proportional to the stator feed frequency, i.e., shaft speed.

$$M(t) = M_o(n) + \Sigma M_z(n)\sin(z2\pi f_v(n)t) \quad (1)$$

With *rotor frequency control*, the frequency of the pulsating torques is proportional to the slip frequency. Hence

$$M(t) = M_o(n) + \Sigma M_z(n)\sin(zs2\pi f_c t) \quad (2)$$

where

- $M(t)$ = time function of the total torque
- $M_o(n)$ = component of torque, which is constant with time but can varry with n
- $M_z(n)$ = amplitude of the harmonic of order z at a given n
- z = pulse number (depending on the system, $z = 6$, 12, 18, etc., or 12, 24, 36, etc.)
- f_c = constant stator feed frequency
- $f_v(n)$ = variable stator feed frequency
- s = slip ($s = (n_s - n)/n_s$)
- n = shaft speed
- n_s = synchronous shaft speed

As will be realized from what has been said, the determination of the pulsating torques requires an extensive knowledge of power electronics and electric motors. The factors involved will be illustrated by means of two examples.

For the first example, the operating conditions (variation of torque and frequency with speed) are shown in Figure 2 for a wound rotor induction motor having a subsynchronous static converter cascade. Two operating ranges are distinguished: the runup and the controlled operation. Runup conditions apply until the lowest controlled operational speed is reached. The behavior in this runup range is just the same as for any normal induction motor whose rotor winding, as in the example, is started through a two-stage resistance. The converter is connected into the rotor control circuit only when the lowest controlled operational speed is reached. At this point, not only the desired drive torque will be developed, but also pulsating torques having six and twelve times the slip frequency. With this drive, six resonance points (marked * in Figure 2) are possible within the operating range, e.g., the value of six times the slip frequency corresponds to the first natural frequency at about 1060 cpm and with the second at about 840 cpm.

The second example has a converter-fed synchronous motor drive, the stator frequency is controlled and, as shown in Figure 3, the conditions are quite different to those in the previous case. The whole of the operation, starting from standstill, is now controlled by the converter. Also in this case, two operating ranges have to be distinguished: pulse operation (n = 0 to 600 cpm) and load commutation (n = 600 to 2850, i.e., 6000 cpm). During the initial pulse operation period, pulsating torques at six

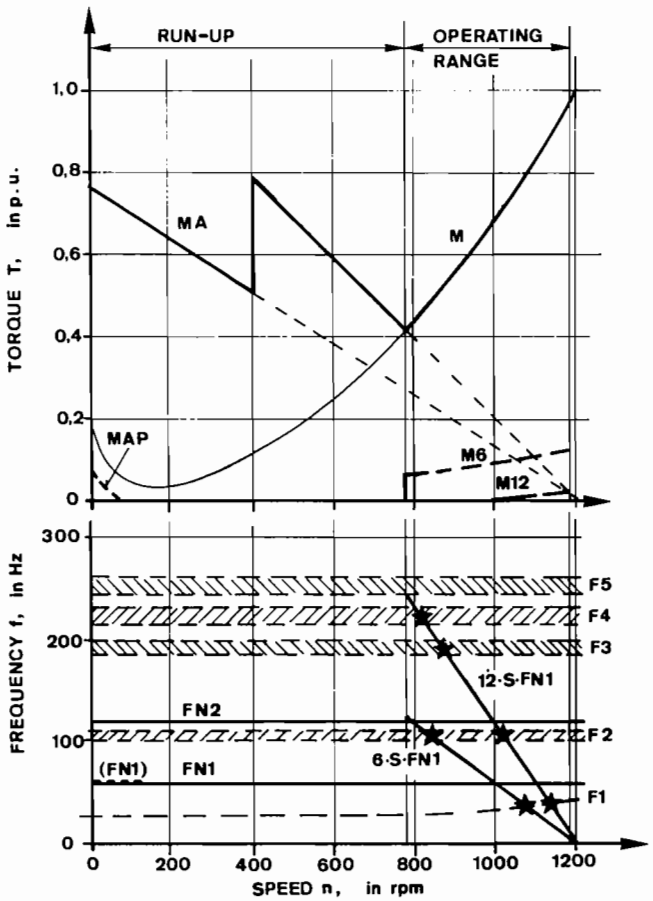

MA Run-up torque with a two-stage resistor
MAP Pulsating part of the run-up torque
M Non-pulsating part of the torque = load torque
M6, M12 Pulsating parts of the torque

EXCITING FREQUENCIES (FN 1 grid frequency: S SLIP)

Run-up	(FN 1)
Operating range	6·S·FN 1; 12·S·FN 1
Electric faults:	FN 1; FN 2 = 2 FN 1

NATURAL FREQUENCIES F 1 to F 5
(system with nonlinear coupling)

Figure 2. Variation of Motor Torque and Exciting Frequency for an Induction Motor with Static Converter Cascade System.

to twenty-four times the stator feed frequency, and having relatively large amplitudes, occur. In load-controlled operation this motor, which has a six-phase stator winding, is subject to pulsating torques having only 12 and 24 times the feed frequency and having moderate amplitudes. With this drive, many resonance points are passed through during runup (0 to 600 cpm: 10 resonance points, 600 to 2850 cpm: 19 resonance points). In the operating range there are two resonance points, at 12 times the stator feed frequency (marked * in Figure 3). As is usual in this kind of calculation, it is assumed that higher natural frequencies are very well damped and are hardly excited. The exciter also causes pulsating torques, but their amplitudes are so small that they may be neglected (the largest amplitude is less than one percent of the rated torque of the synchronous motor).

Other types of drive systems which are listed in Table 2 can show much more complicated relationships [11, 12, 13]. In each case, it is advisable to discuss the problem thoroughly with a

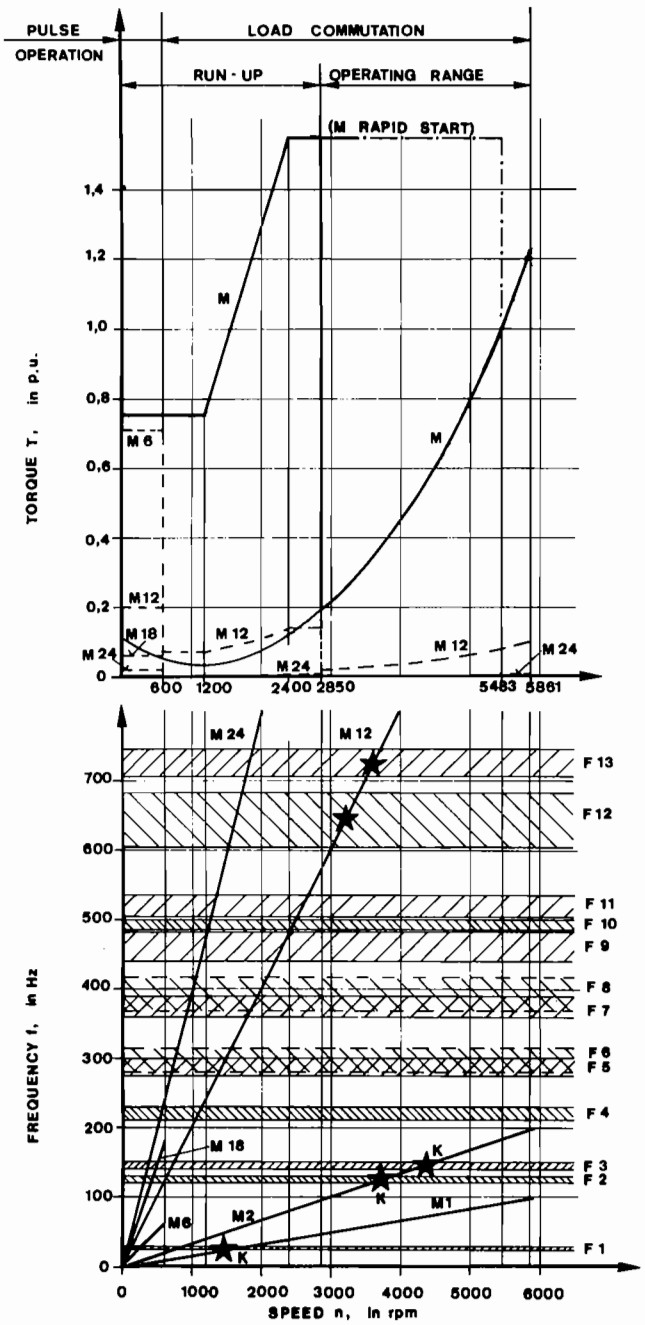

M	Non-pulsating part of the torque (highest possible value)
M6, M12, M18, M24	Pulsating part of the torque

EXCITING FREQUENCIES

Pulse operation	M6, M12, M18, M24
Load commutation	M12, M24
Electric faults	M1, M2 = 2M1

NATURAL FREQUENCIES F1 to F13

Figure 3. Variation of Motor Torque and Exciting Frequency with Speed for a Converter-fed Synchronous Motor Drive.

specialist in order to avoid any unneccessary operating difficulties which may result from a false interpretation of the operating behavior.

ELECTRICAL FAULT TORQUES

In order to ensure the high availability which is required of these drives, one must also be able to calculate their behavior under possible electrical fault conditions, of which there are a number. The plant owner is seldom in a position to define the actual "worst case," and, on the other hand, it is hardly possible to extend the calculations to cover all possible cases. As an effective measure in this situation, it has become accepted practice to check the electric drives for "short-circuit safety" [14, 15]. For this purpose, the phase-to-phase terminal short-circuit torque at voltage zero (crossover) is used. In a simplified analytical form, we have:

$$M_{2K}(t) = M_K \left[e^{(t-t_o)/T_1} \sin 2\pi f_1 (t-t_o) - 0.5e^{(t-t_o)/T_2} \sin 4\pi f_1 (t-t_o)\right] (t \geq t_o) \quad (3)$$

where

$M_{2K}(t)$ = time function of two-phase terminal short circuit
M_K = torque amplitude
f_1 = stator feed frequency (with stator frequency control, $f_1 = f_v(n)$; with rotor frequency control, $f_1 = f_c$).
T_1, T_2 = time constants
t_o = instant of occurrence of fault

In the example of the induction motor in Figure 2, the Campbell Diagram shows that the worst short-circuit case occurs at maximum speed. This results from the fact that a non-linear coupling is installed in the shaft line. With increasing speed, i.e., static torque, the stiffness of the coupling increases, hence causing an increase in some of the natural frequencies. The first natural frequency F1 is therefore the next closet to the simple stator supply frequency FN1 at maximum shaft speed.

With the synchronous motor (Figure 3), the conditions are much more involved. In the operating range, at about 3650 cpm and at about 4400 cpm (marked * with a K in Figure 3), double the stator feed frequency corresponds to the second and third natural frequencies, respectively. This means resonance. For safety's sake, a short circuit at about 1600 cpm should also be checked for this drive. At this speed, the first natural frequency is in resonance with the simple stator feed frequency.

CALCULATION MODEL FOR THE SHAFT LINE

Reliable calculation results are possible only when exact data regarding the exciting torques are used and also when the model of the shaft line correctly reflects the mechanical characteristics of the design. As a result of many years experience in this field, the "Method of Two Limit-Cases" has been developed. The principles of this method are outlined in Table 3, and Figure 4 shows all possible situations in regard to the calculation results. It can be seen that the scatter bands for torques in the individual shaft parts can have very different values. When using the conventional calculation method, which makes only one estimate of the model, a much larger allowance must be added (e.g. $\pm 5\,\Delta T_1$) in order to achieve the same security in the calculation results, because the allowance must cover the worst case represented in the Two Limit-Case Method. Large safety margins should be avoided, because they can lead to unneccessary design modifications. The results presented show that the extra calculation labor for the Method of Two Limit-Cases is well justified.

Table 3. Calculation of Torsional Oscillation for the Shaft Line Using the Method of Two Limit-Cases.

ASSUMPTIONS FOR EACH ELEMENT OF THE SHAFT LINE USED IN THE METHOD OF TWO LIMIT-CASES

(Element: Part of shaft with constant torsional stiffness
FE-program input: length ≤ equivalent diameter)

	SPRING CONSTANT	MASS MOMENT OF INERTIA
1	AS FLEXIBLE AS POSSIBLE	LARGEST POSSIBLE VALUE
2	AS STIFF AS POSSIBLE	SMALLEST POSSIBLE VALUE

DAMPING: conservative values
EXCITING: significant upper limit values

ADVANTAGES

- Assumptions for stiffness simple and clearly interpretable
- The available spread of the mass moment of inertia is covered
- Actual natural frequencies will be straddled
- Torques in the shaft parts are defined limit values (Fig. 4)
- For cumulative damage calculations, the higher of the calculated shaft torques has a very high confidence limit.

DISADVANTAGES

- Two parallel calculations must be made for each load case

Exception: In cases of resonance, calculation with only the flexible case assumption is sufficient.

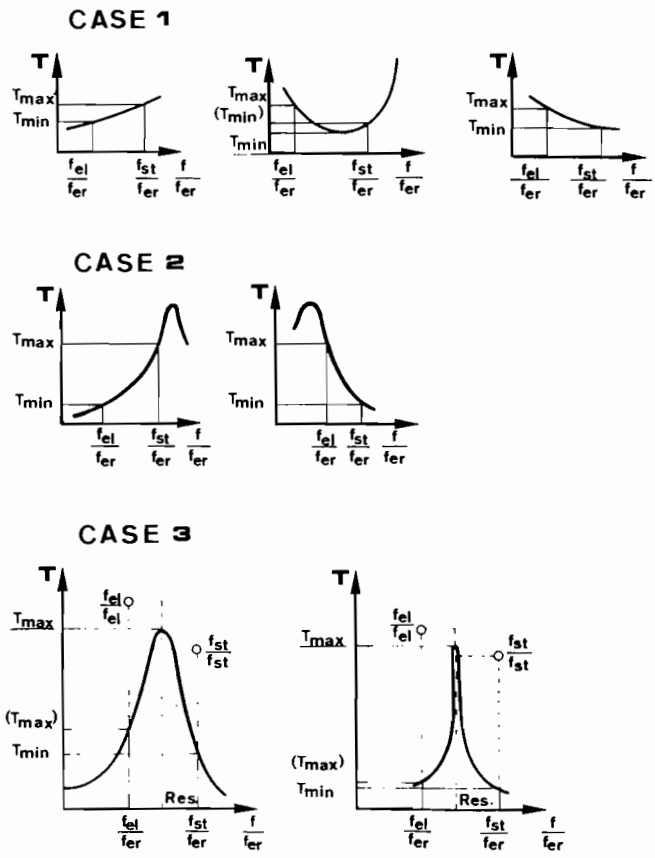

Case 1: Exciting frequency far enough from natural frequency
$\triangle T_1 = T_{max} - T_{min}$

Case 2: Exciting frequency near a natural frequency
$\triangle T_2 = T_{max} - T_{min} \approx (2 \text{ to } 3) \triangle T_1$

Case 3: Exciting frequency straddled by a natural-frequency scatter-band
$\triangle T_3 = T_{max} - T_{min} \approx (4 \text{ to } 7) \triangle T_1$

f_{er} : exciting frequency
f_{el} to f_{st}: natural frequency scatter-band
T : torques on the shaft

Figure 4. Discussion of Possible Results of Torsional Oscillation Calculations Made Using the Method of Two Limit-Cases.

In the determination of the mass moments of inertia, there are also objective uncertainties which cannot be ignored. With case pump impellers whose flow passages are not machined, scatter ranges of about five percent may result from casting tolerances. In addition, there are as yet no reliable data regarding the amount of the water mass participating in the oscillation [16, 17]. The rough rule used—calculate either with all the water in the impeller or with no water in it—fits very well into the Two Limit-Case concept. The rotors of electrical machines having a laminated core also have deviations due to fabricating tolerances (± 2 percent). Other types of machines are outside the scope of this paper.

Compared with fluid flow machines, determining the torsional stiffness of rotors for electrical machines is not exactly straightforward, since the latter cross-sections are usually not purely annular, and are often not in one piece. (The torsional resistance and the polar moment of inertia are numerically equal only with annular cross-sections). Appendix A shows how the torsional stiffness is determined for two common rotor geometries.

CALCULATION MODEL FOR DAMPING

With variable-speed electric drives, a number of calculations must be made to cover passing through the resonance points or steady operation at a resonance point. This requires an input of data regarding the damping, particularly damping in the mechanical system. By virtue of its simplicity of mathematical treatment, practically only the velocity-proportional damping is used in engineering calculations. The mathematical treatment of damping in the equations of motion is given in *Appendix B*.

Basically, we can distinguish between the various kinds of damping, as follows:

- internal damping where we distinguish between
- material damping
  - in steel parts of the shaft line
  - in the elastometric elements of flexible couplings
- structural damping
  - at mating surfaces of rotor parts
- external damping
  - damping through the surrounding medium e.g., water, air, electromagnetic field in the air gap

For torsional oscillation calculations, the internal damping (material and structural damping can be assumed as:

$$Q_K = 100 \quad (\zeta = 0.5\%) \tag{4}$$

The value to be used for the external damping is a subject of dispute. For pump impellers, there are as yet no proven methods for calculating the torsional damping accurately. A rough approximation, which is often used, is given in *Appendix C*.

Where elastic couplings are installed, they provide a large part of the damping. Depending on the design and the quality of the elastic material used, values of

$$Q_K = \text{from 20 down to 5 } (\zeta = 2.5 \text{ to } 10\%) \qquad (5)$$

can be obtained. It must be realized that the use of these couplings at higher speeds (n > 3000 cpm) and power ratings is limited. The use of an element having a high damping capacity is the simplest way to keep the resonance oscillations at a low value.

EXAMPLE: BOILER FEED PUMP DRIVEN BY STATIC CONVERTER-FED SYNCHRONOUS MOTOR

The principal results of a torsional vibration calculation for an actual installation are set out below. The iterative solution method is shown schematically in Table 4.

Physical System/Model

The plant configuration and the FE model employed for the entire shaft line are shown in Figure 5. The rotor model has a total of 92 torsional degrees of freedom.

All computer calculations were performed with the MADYN machine dynamics program [18, 19].

Table 4. Solution Method Scheme.

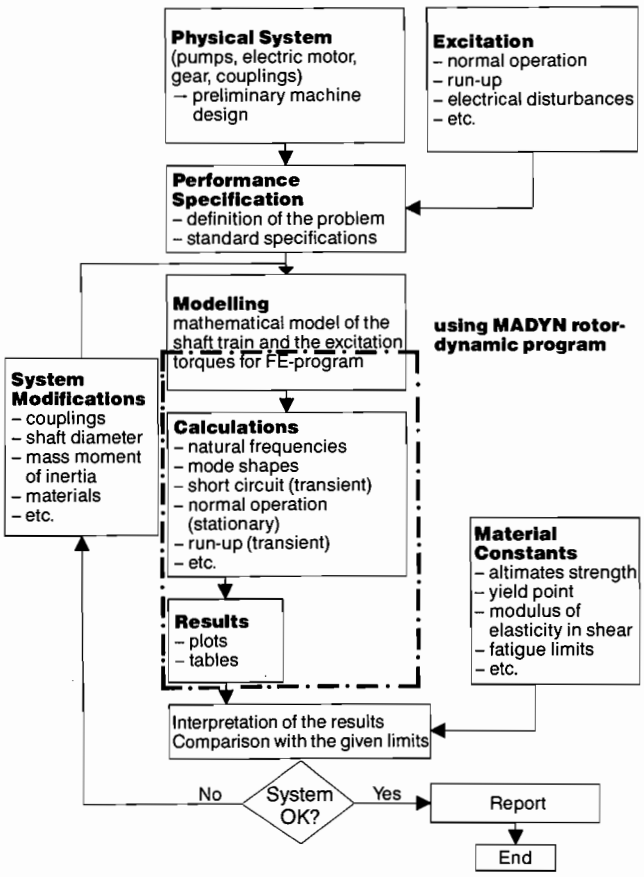

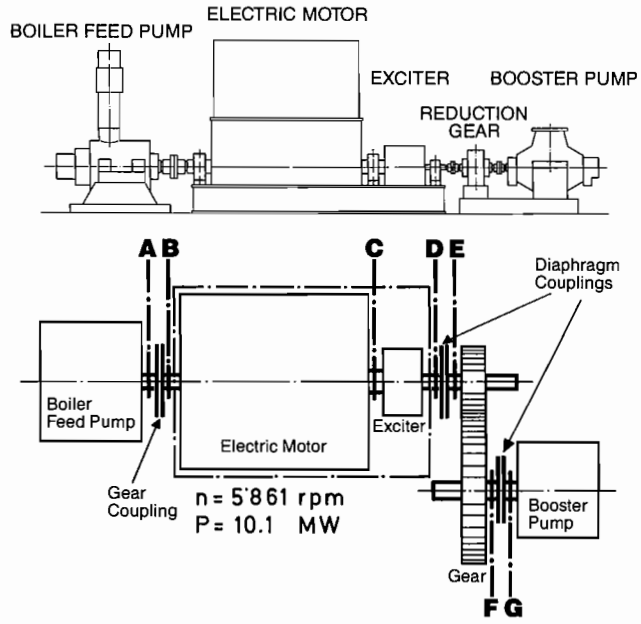

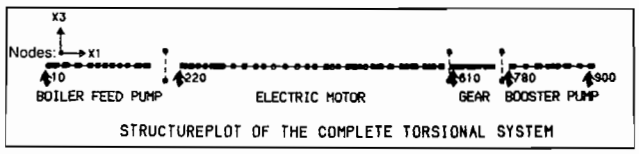

Figure 5. Feed Pump Set; Shaft System and Mathematical Model of the Complete Shaft Train.

Calculations

First the relevant torsional natural frequencies and the associated mode shapes were calculated. The mode shapes are plotted in Figure 6. The normalized angle of rotation of the nodes is represented as a translatory deflection.

After this, the maximum torques and stresses in the critical cross-section A to G (Figure 5) were calculated for the possibly critical torsional short-circuit speeds. The transient responses of the torsional stresses in a few short circuit cases are plotted in Figure 7. A more accurate investigation revealed that at a speed n = 4434 cpm (= 0.5 × F3) the worst possible short circuit case would occur. In all calculations of the forces vibrations, a modal damping of ξ = 1 percent for the 16 lowest mode shapes was generally assumed (Quality factor Q = ½ξ = 50).

All relevant continuous operating conditions were likewise checked, by abruptly introducing the corresponding excitation torque M(t) resulting for the particular operating point, and following the transient response over the time range. This procedure yields information on the decay of disturbances and the steady-state condition which is reached corresponds to the desired steady-state solution.

The torsional vibrations in continous (steady-state) operation at maximum speed (n = 5861 cpm) is shown by way of example in Figure 8. The maximum dynamic torques, however, will occur at a lower shaft speed (≈ 3530 rpm), when M12 excites the 13th mode F13 (see Figure 3).

Here, maximum dynamic torques will take place at section B (see Figure 5). However, this dynamic torque does not exceed 0.25 percent of the static torque.

One can conclude that the steady-state dynamic torques in the normal operating range are "filtered out" by the heavy mass moment of inertia of the motor rotor.

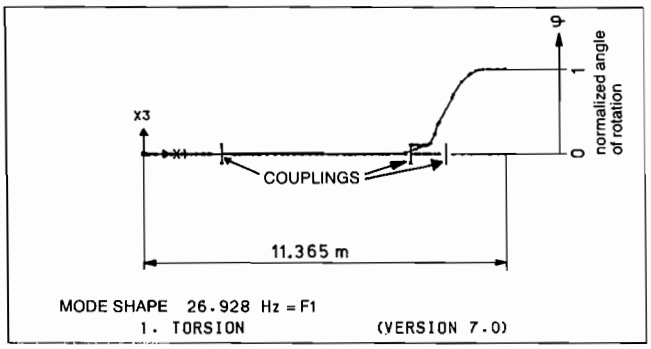

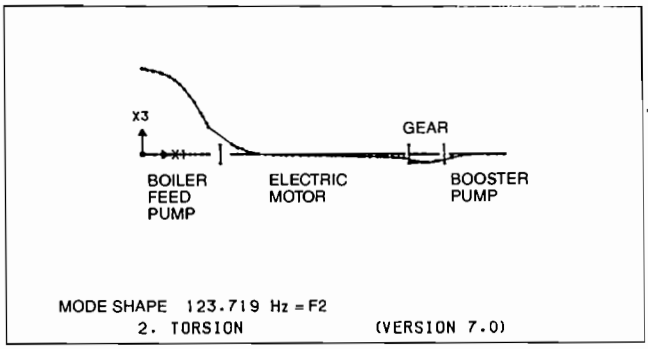

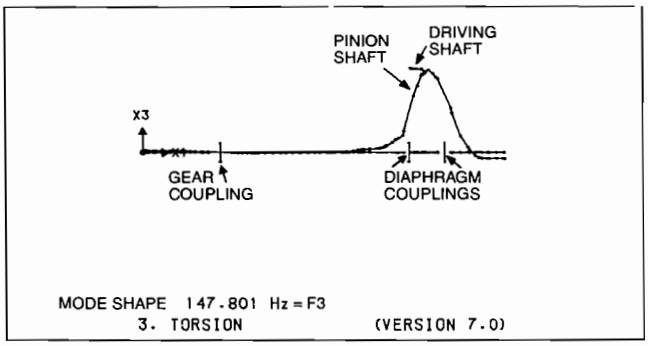

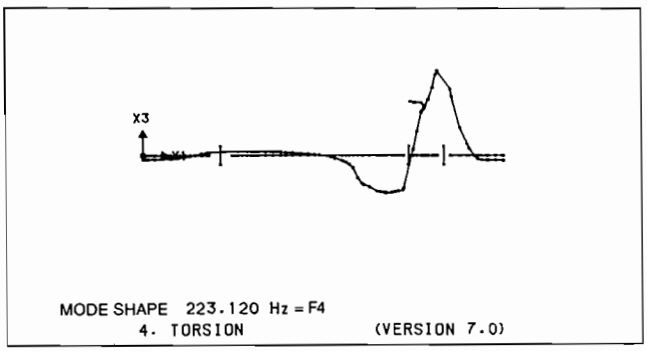

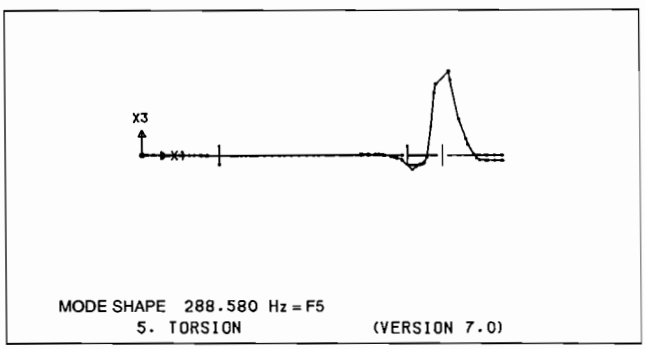

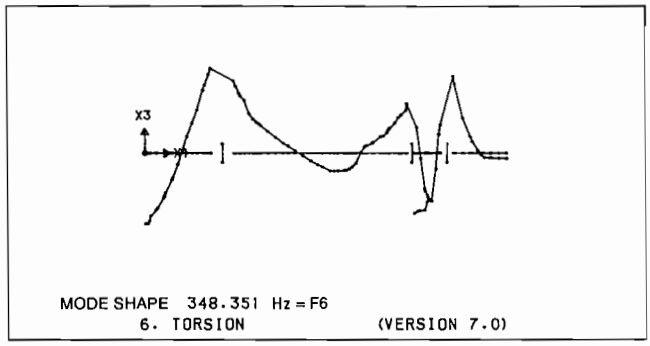

Figure 6. Torsional Mode Shapes.

Another very important dynamic load case is the run-up of the unit in the pulse operation range (here 0 to 600 cpm). Realistic simulation of the transient excitation requires a relatively complex computer program. The MADYN program is capable of taking into account the change in frequency and amplitude of the excitation torque with time (Equation (1)). When passing through torsional critical speeds, the harmonic components of the exciting torque (see Figure 3, M6 . . . M24) set up considerable torsional stresses in the endangered cross-sections; the admissibility of these must be verified without fail. It must also be ascertained whether any transmission elements having backlash, such as gears and gear-type couplings, lift off due to torque reversals. The resulting dynamic torsional stresses and torques for two different shaft cross-sections are plotted in Figure 9.

Comments on the Results

- From the torsional mode shapes (Figure 7), it is immediately apparent that up to about 150 Hz the two substructures—main pump and its motor and booster pump, gearing and motor—may be regarded as virtually independent systems.
- For the electrical fault case of a phase-to-phase short circuit across the terminals, n = 4434 cpm was found to be the torsionally critical speed. The double stator feed frequency (see Equation (2)) excites the third natural frequency F3, chiefly at this operating speed (Figure 7). Yet even this highly improbable disturbance does not impose inadmissible stress states on the shaft line (τ_{max} = 150 N/mm^2).

All continuous operating states (operation range) show negligible dynamic load values in the steady-state, because in the load commutating operation (here n > 600 cpm) practically no significant dynamic torque amplitudes occur, or only with a relatively high-frequency excitation with the 12th and 24th speed order (Figure 3 and Equation (1)).

- The loads vs. time curves plotted in Figure 9 show the behavior of the shaft line immediately after switch-on, and when passing through the first torsional critical speed F1, which is excited mainly by the 6th harmonic of the pulsating torque.

In addition, it can also be shown that with the estimated modal torsional damping ξ = 1 percent, the gear-type coupling between the motor and the feed pump sustains no torque reversals. On the other hand, the two couplings to the gear unit (booster pump side) must be selected for the brief torque reversals imposed. Because for gear couplings this would mean "hammering" on the coupling teeth, diaphragm couplings have been selected.

SELECTION OF COUPLINGS

In addition to the torsion analysis results, further criteria have to be taken into account when selecting the couplings. These

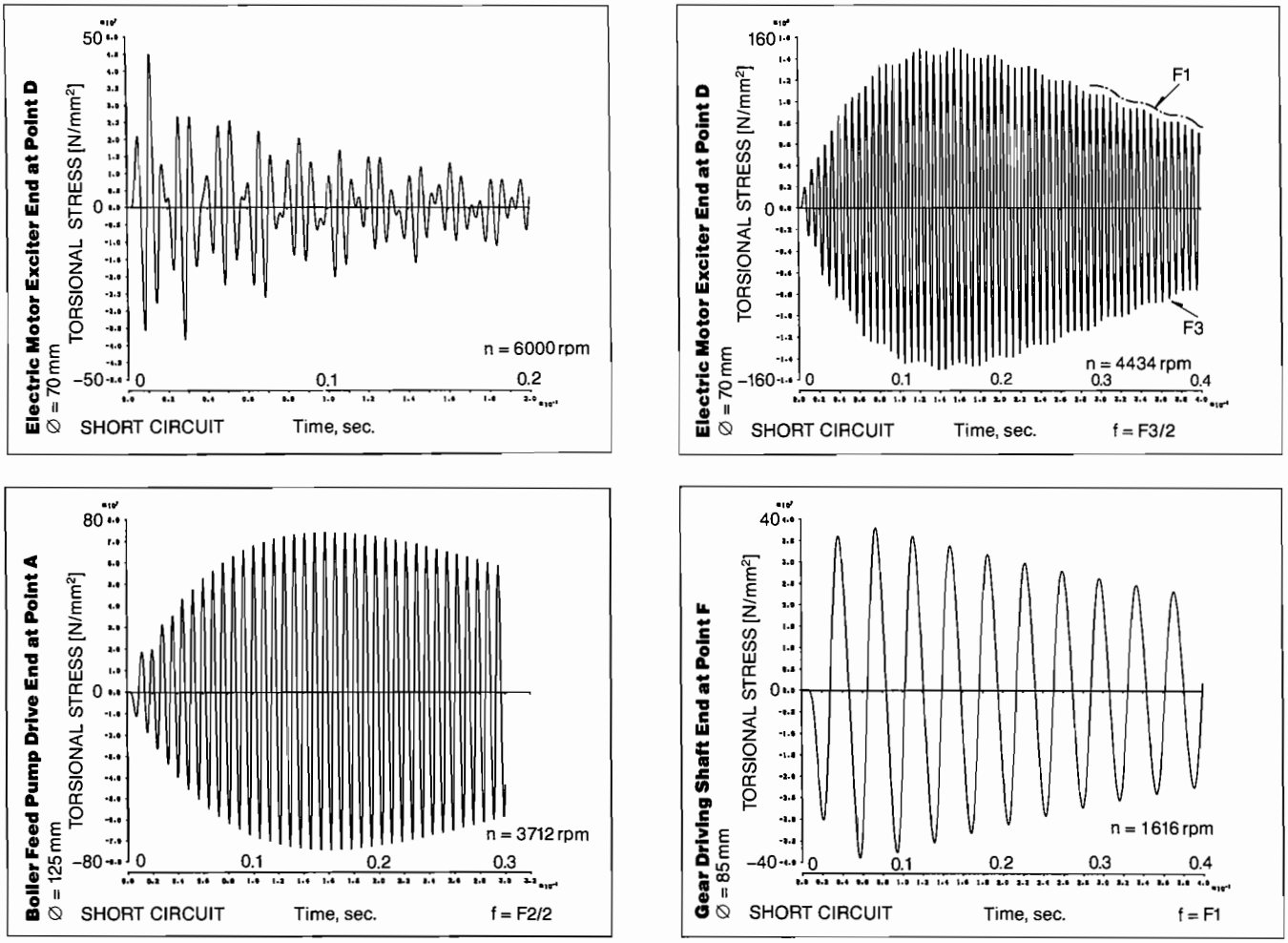

Figure 7. Phase to Phase Short Circuit Across the Terminals.

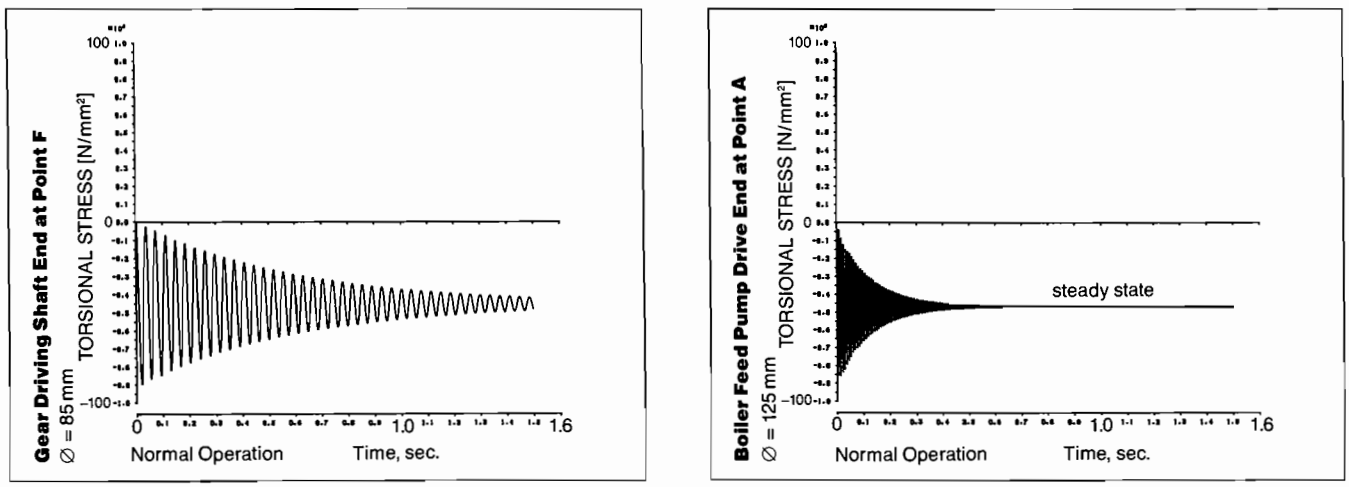

Figure 8. Normal Operation at n = 5861 cpm (→ Steady State).

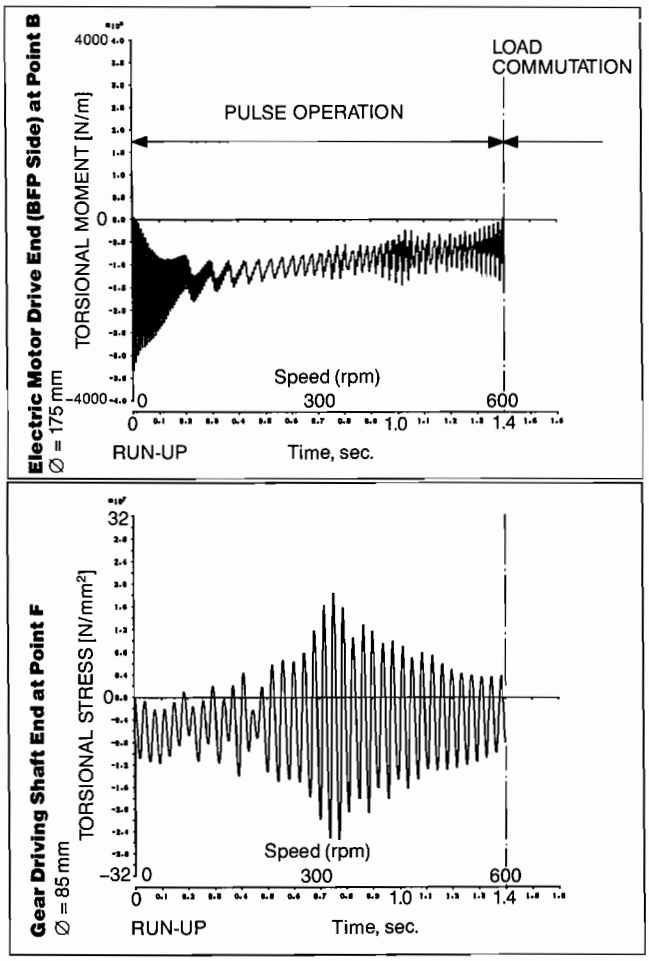

Figure 9. Run-up at Pulse Operation (n = 0 ÷ 600 cpm).

include running behavior, axial extensions, take-up of axial forces and line-up of the shaft train.

The selection criteria for the couplings arising from the torsion analysis were described. Further, comprehensive investigations are required in order to evaluate the lateral running behavior. These do not form part of the present report. The effects of axial extensions and axial forces on the couplings, as well as the lining up of the shaft train, are influenced by further design and operating factors.

The actual shaft system with the selected couplings is shown in Figure 10. For reasons of high power and high shaft speed present in this pump set, all-metal couplings have been foreseen. Between the motor and the feed pump, a *gear coupling* has shown to be advantageous. The coupling is lightweight and allows for higher lateral critical speeds.

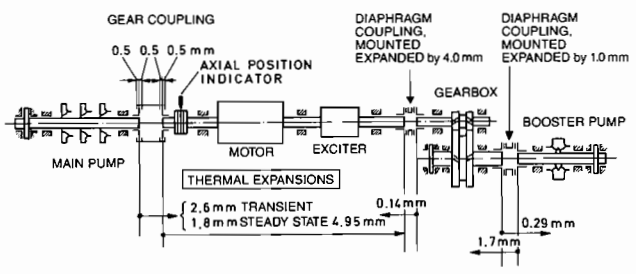

Figure 10a. Rotor Positioning and Thermal Expansion.

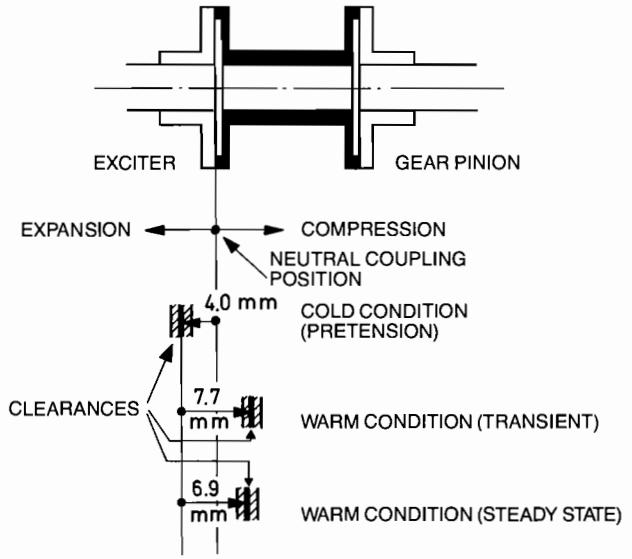

Figure 10b. Situation at Coupling Between Exciter and Gearbox: Relative Position of Exciter Shaft End vs. Pinion.

Additionally, the type selected with limited end float provides for good axial guidance of the motor/exciter rotor which has in this case no thrust bearing.

Between exciter and gearbox, as well as between gearbox and booster pump, *diaphragm type couplings* have been foreseen. The main reason for this selection is the resultant torque reversal during start-up in the "pulse operation" range (previously mentioned).

However, the diaphragm coupling between exciter rotor and gear pinion has to take all thermal expansions of feed pump rotor, motor/exciter rotor and gear pinion as shown in Figure 10b.

Therefore, a slightly oversized coupling had to be selected at this location to allow for the expansions in question without endangering long term operation. The coupling will be prestressed in tension in the cold condition.

A lightweight design with a titanium hub on the pinion side was chosen in order to increase the lateral critical speed of the pinion.

CONCLUSION

With torsional oscillations, the danger of a shaft failure is much greater than with flexural vibration. In summary, however, it can be said that with good, close cooperation between the manufacturers of each of the machines used in the unit, and between them and the plant owners, the problem of torsional oscillation of variable-speed electric drives can be safely brought under control with the help of the calculation methods now available. As a very efficient aid in reducing the stresses in the shaft line, damping elements (flexible energy-absorbing couplings, dampers) can be installed.

Additional research effort will be needed in order to consider the contribution of pump impellers to torsional damping. Few experimentally confirmed data exist yet, especially for impellers which are oscillating in torsion.

APPENDICES

Appendix A

As an introduction, the familiar case of a rigidly fitted coupling (Figure A-1) will be shown. In the case denoted "as flexible as possible," it is assumed that the force flow is through the smallest possible cross-section of the shaft elements. In the case denoted

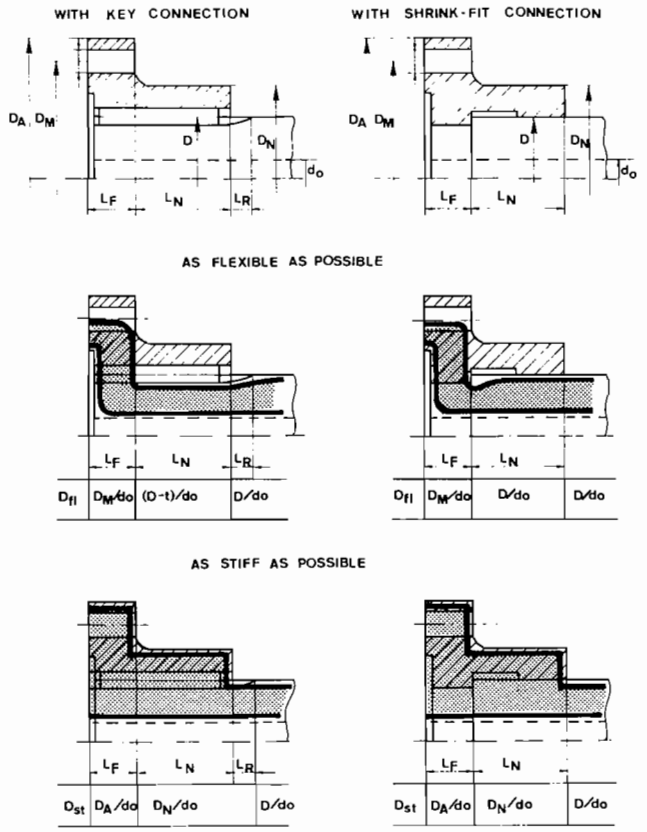

Figure A-1. Application of the Method of Two Limit-Cases to a Torsionally Stiff Coupling Having Either Keyed or Shrink-Fit Design.

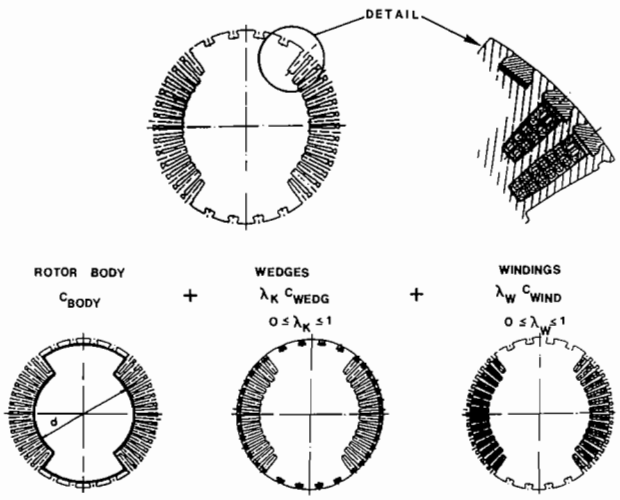

Flexible assumption

$D_{Ael} = 0.98\, d\, \kappa_{TA}$

Stiff assumption

$$D_{Ast} = 1.05\, d \sqrt[4]{\kappa_{TA}^4 + 8\frac{E_K}{E_R}\frac{h_K}{d}\left[1 + 6\frac{H_N}{d} + 12\left(\frac{H_N}{d}\right)^2\right]}$$

Figure A-2. Torsional Stiffness of a Synchronous Motor Rotor Body Cross-Section.

"as still as possible," the outer contours of the shaft sections are considered. This will lead to an understanding of the more complicated cases with electrical machines.

In Figure A-2, it is shown how the torsional stiffness of a cross-section of the cynlindrical rotor of a two-pole synchronous-motor can be determined. There are three components: one from the cross-section of the rotor body, one from the wedges which are pressed against the wedge slots by the centrifugal force (the force is transmitted partly by friction), and one from the windings. For the Two Limit Models (one "as flexible as possible"—rotor body cross-section only and the other "as stiff as possible"—includes wedge and winding contribution), the relevant equations are shown in Figure A-2. Figure A-3 shows the coefficients $_K$ for calculating the equivalent diameter of the rotor body cross-section. The difference between the torsional resistance and the polar moment of inertia for the rotor body cross-section is shown in Figure A-4.

Figure A-5 shows how the torsional stiffness of a ribbed shaft is determined (the rotor core is attached to the outer edge of the ribs).

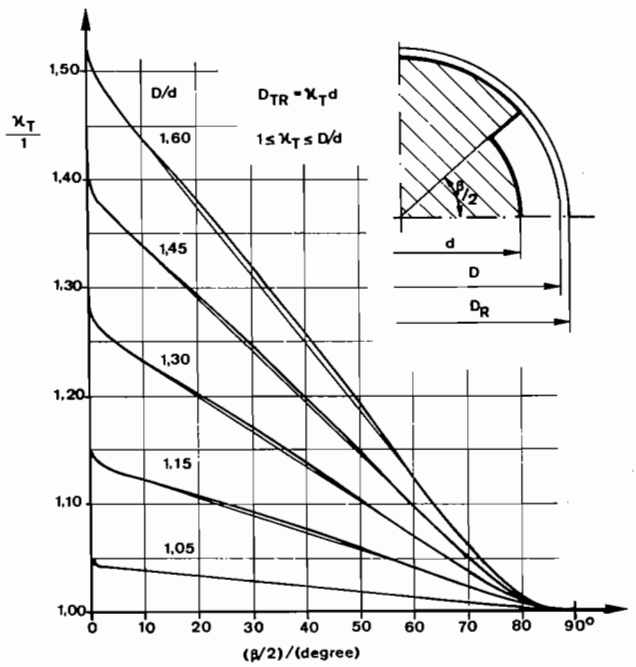

I_T: torsion constant of cross-section $I_T = 4 \oint \phi \, d\, A$

I_P: polar moment of inertia for the reference cross-section $I_P = \pi\, d^4/32$

D_R: rotor outside diameter

D: effective rotor outside diameter

d: diameter of the circle described by the slot bottom

D_{TR}: equivalent diameter for torsion

Figure A-3. Equivalent Diameter for the Torsional Stiffness of a Two-Pole Synchronous Motor Rotor Body Cross-Section Calculated with BEM Program in Accordance with the Saint-Venant's Theory.

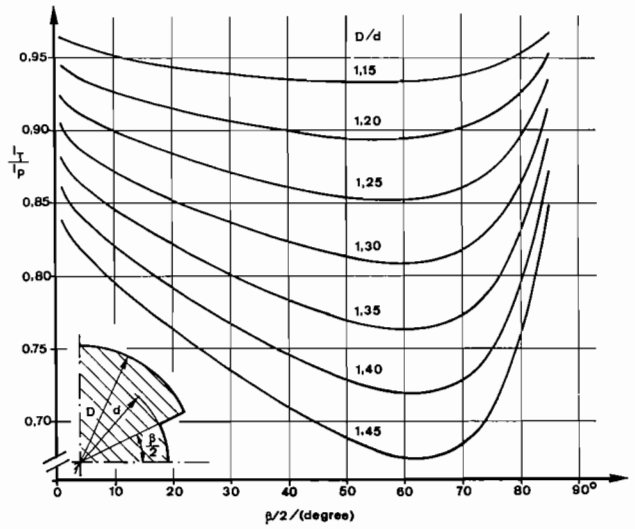

I_T: torsion constant of cross-section $I_T = 4 \oint \phi \, d\, A$

I_P: polar moment of inertia $I_P = \frac{\pi}{32} D^4 - \frac{\pi}{32}(D^4 - d^4)\frac{\beta}{180}$

For turbomotors: $D/d \leq 1.45$; $40° \leq \beta \leq 65°$

Figure A-4. Torsion Constant for a Two-Pole Synchronous Motor Rotor Body Cross-Section in Relation to the Polar Moment of Inertia.

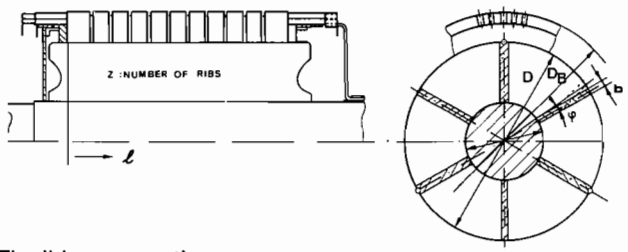

Flexible assumption

$$\frac{1}{c} = \frac{32l}{\pi G D^4_{eq}} = \frac{1}{c_{mid}} + \frac{1}{c_{rib}}$$

$$D_{eq} = \frac{d}{\sqrt[4]{1 + \frac{\pi}{32(1+\upsilon)}\left(\frac{D}{d}-1\right)^3 z\left(\frac{l}{d}\right)^2\left(\frac{D}{d}\right)^2\left(\frac{b}{d}\right)^3}} \qquad (D_{eq} \leq d)$$

$$D_{el} = 0.98\, D_{eq}$$

Stiff assumption

$$D_{st} = \sqrt[4]{D^4_{eq} + (D^4_B - D^4)/\lambda}$$

$\lambda = 100$ to 1000

Figure A-5. Torsional Stiffness of Ribbed Shafts for Electrical Machines.

Appendix B

The n coupled differential equations of motion for a system with n degrees of freedom are, in matrix notation as follows:

$$M\ddot{X} + D\dot{X} + KX = F \qquad \text{(B-1)}$$

where

M = mass matrix (diagonal)
D = damping matrix
K = stiffness matrix (symmetrical, tri-diagonal)
F = load matrix
X = coordinate of motion

For various calculation operations it is convenient when the damping matrix is also symmetrical and consists of a linear combination of the mass and the stiffness matrix, as Rayleigh recommended:

$$D = \frac{\omega^x}{Q_M} M + \frac{1}{Q_K \omega^x} K \qquad \text{(B-2)}$$

where [20]

Q_m = quality factor for absolute damping, i.e., external damping
Q_k = quality factor for relative damping, i.e., material damping
ω^x = resonance angular velocity

With these resonance calculations, a different quality factor can be considered for each resonance point. It is also possible to make calculations without either Q_M or Q_K. If the program uses a numerical method for solving the differential equations, e.g., the Runge-Kutta method, one can also consider a different Q_M and/or Q_K for each individual section of the shaft. This method also permits the consideration of shaft elements having non-linear stiffness.

If the program uses the modal analysis procedure, then the equations of motion are decoupled by multiplication with the modal matrix o, which can be obtained from the hommogeneous equation system without damping (weak damping: $\rightarrow MX + KX = 0$).

$$\phi^T M \phi \ddot{Y} + \phi^T D \phi \dot{Y} + \phi^T K \phi Y = \phi^T F \qquad \text{(B-3)}$$

The decoupled equations can be expressed in normal coordinate form as:

$$\ddot{y}_i + (2\zeta_i \omega_i)\dot{y}_i + \omega_i^2 y_i = \bar{f}_i(t) \quad i = 1,2,\ldots n \qquad \text{(B-4)}$$

The modal damping, which is

$$\frac{1}{Q_i} = 2\zeta_i = \frac{\alpha_i}{\omega_i} + \beta_i \omega_i \qquad \text{(B-5)}$$

can be expressed differently for each eigenvalue ω_1.

Appendix C

Figure C-1 shows the torque/speed curve of M(ω), from which the torsional damping can be estimated as follows:

$$M(\omega) = M_{oo} \cdot \frac{n^2}{n_{oo}^2} = M_{oo} \cdot \frac{\omega^2}{\omega_{oo}^2} \qquad \text{(C-1)}$$

where

$M(\omega)$ = torque at actual speed
M_{oo} = torque at rated speed
n_{oo} = rated shaft speed
ω_{oo} = rated angular velocity of the shaft
n = actual shaft speed
ω = actual angular velocity of the shaft

The damping constant is calculated as:

$$d \cong \frac{dM}{d\omega} = \frac{2M_{oo}}{\omega_{oo}} \cdot \frac{\omega}{\omega_{oo}} \qquad \text{(C-2)}$$

It is apparent that the absolute damping is dependent on the actual running speed.

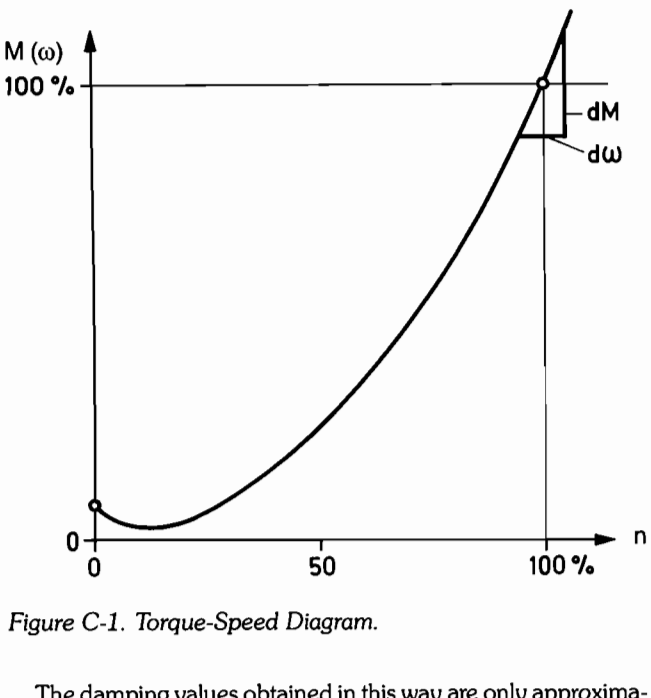

Figure C-1. Torque-Speed Diagram.

The damping values obtained in this way are only approximations, because they are taken from a static characteristic. Effectively, however, the damping mechanism is a dynamic process.

Tests will have to be carried out to obtain experimental values for these damping constants.

REFERENCES

1. Kessler, G., "Entwicklung der elektrischen Antriebstechnik in den letzten 20 Jahren," Antriebstechnik *20*, pp. 187-191 (1981).
2. Skudelny, U.-Chr, "Stand und Entwick-lungstendenze drehzahlgeregelter Antriebe," VDE-Tagung, Drehzahlgeregelte Antriebe Haus der Technik, Veröff. *499*, pp. 4-12 (1981).
3. Stemmler, H. and Meyer, A., Brown Boveri Review *69* (4/5), pp. 114-121 (1982).
4. Meier, U., "Möglichkeiten des Regelns von Drehstromantrieben," Maxhinenemarkt *91*(59), pp. 1133-1136 (1985).
5. Barker, B., "Variable Speed Converter Drives for Power Station Auxiliaries," IEE International Conference on Electric Machines, IEE Publication No. 213, pp. 152-153 (1982).
6. Shilston, P.D., "Variable Speed Pump Drives—The Way Ahead," 8th Conference British Pump Manufacturers Association (1983).
7. Brunner, H., "Die Vorteile überwiegen. Betriebserfahrungen mit Drehstrom-Regelantrieben," Elektrotechnik *66*(11), pp. 21-25 (1984).
8. Hickok, H.N., "Adjustable Speed—A Tool for Saving Energy Losses in Pumps, Fans, Blowers, and Compressors," IEE Trans. Ind. Appl. IA-21, *1* pp. 124-136 (1985).
9. Urano, A.S., and Appiarius, J.C., "System Benefits and Considerations when Using AC Adjustable Frequency Drives in Generating Stations," American Power Conference, Chicago, Illinois (1981).
10. Wild, M., and Wetzel, R., "Stromrichter-Synchronmotoren im Krafwerk Bergkamen, zum Antrieb von Kesselpumen," VDE-Tagung Drehzahlgeregelte Drehstromantriebe, Haus der Technik, Veröff. *449*, pp. 55-58 (1981).
11. Andersen, E. Ch., Bieniek, K., and Pfeiffer, R., "Pendelmomente mit Wellenbeanspruchungen von Drehstrom—Käfiglaufmotoren bei Frequenzumrichterspeisung," ETZ-Archiv *45* (1), pp. 25-33 (1982).
12. Harders, H. and Weidemann, B., "Pendelmomententwicklung bei der stromrichtergespeisten Asynchronmaschine mit Berucksichtigung des welligen Zwischen-kreisstromes," Arch. F. Electrotechnik *64*, pp. 294-305 (1982).
13. Case, M.J., "Torque Pulsation in Current-Source Inverter Induction Motor Drives," Arch. f. Eletrotechnik 66, pp. 111-115 (1983).
14. DIN 57530/Teil 3 (VDE 0530, Teil 3) Beuth-Verlag, Berlin, p. 5 (1978).
15. Koglek, H., "Kurzschlussprobleme bei rotierenden Machinen," E. und M. *102*(718), pp. 278-291 (1985).
16. Blevins, R.D., "Formulas for Natural Frequency and Mode Shape," Van Nostrand Reinhold Company, New York (1979).
17. Liu, W.K., Lam, D., and Belytschko, T., "FEM for Hydrodynamic Mass with Nonstationary Fluid," Comp. Meth. Appl. Mech. Engng. *44*, pp. 1772211 (1984).
18. Klement, H.D. and Merker, H.J., "Description of MADYN," Engineering Office Klement, Alkmaarstrasse 13, D-6100 Darmstadt 13 FRG.
19. Kramer, E., "Maschinendynamik," Springer, Berlin, p. 354 (1984)
20. Timoshenko, T., Young, D.H. and Weaver, Jr., W., *Vibration Problems in Engineering*, 4th Ed., New York: John Wiley and Sons p. 344 (1974).